Period-doubling cascades and chaos in a semiconductor laser with optical injection

T. B. Simpson
JAYCOR, P.O. Box 85154, San Diego, California 92186-5154

J. M. Liu
Department of Electrical Engineering, University of California, Los Angeles, Los Angeles, California 90024-159410

A. Gavrielides, V. Kovanis, and P. M. Alsing
Nonlinear Optics Center, Phillips Laboratory, PL/LIDN, Kirtland Air Force Base, Albuquerque, New Mexico 87117-5776

(Received 30 September 1994)

We characterize the nonlinear dynamics of a semiconductor laser subject to optical injection. The key characteristics of measured optical spectra are reproduced in calculations based on a single-mode model that includes spontaneous-emission noise. The laser exhibits chaos over a bounded range of injection levels. As the chaotic regime is approached from both lower and higher injection levels, a period-doubling route to chaos is followed, although the route is obscured by spontaneous-emission noise. A new, bounded regime of period-doubling occurs for injection levels well above the region of chaotic dynamics. Optical injection strongly modifies the carrier-field resonance coupling frequency.

PACS number(s): 42.55.Px, 05.45.+b

Nonlinear dynamics in semiconductor lasers is the subject of considerable current research [1]. It was predicted [2], and recently confirmed [3], that external optical injection in a semiconductor laser can lead to chaos through a period-doubling route. Because of the very short time scales (subnanosecond) on which the dynamics occurs, measurements of the output spectrum must be combined with model calculations in order to extract information about the properties of the nonlinear dynamics [2–5].

In this paper, experimental measurements and calculations based on a single-mode model are combined to give a consistent picture of nonlinear dynamics in a laser diode. We show that a laser diode under optical injection at its free-running frequency exhibits a region of chaotic dynamics that is bounded as a function of the injection level, and that the laser follows a period doubling route to chaos as the injection level is varied from *both* above and below [6]. Spontaneous emission into the oscillating mode acts as an additional, fluctuating optical input which broadens and obscures features of the period-doubling cascades. At high injection levels we observe a distinct period doubling which does not proceed to further bifurcations and chaos. The existence of a second, distinct period-doubling region has not, to the best of our knowledge, been previously reported in a semiconductor laser subject to optical injection.

A single-mode model of a semiconductor laser under external optical injection can be cast in a form which emphasizes key dynamic parameters [3]:

$$\frac{da}{dt} = \frac{1}{2}G(1+a) + \eta a_i \cos(\Omega t + \phi) + F'/|A_o|, \quad (1)$$

$$\frac{d\phi}{dt} = -\frac{b}{2}G - \frac{\eta a_i \sin(\Omega t + \phi) - F''/|A_o|}{1+a}, \quad (2)$$

$$\frac{d\tilde{n}}{dt} = -\gamma_s \tilde{n} - \frac{\gamma_s}{\gamma_c}\tilde{J}G(1+a)^2 - \gamma_s \tilde{J}(2a+a^2). \quad (3)$$

Here, $a = (|A|/|A_0| - 1)$ and $a_i = |A_i|/|A_0|$, where $|A|$ is the magnitude of the slave laser oscillating field, $|A_0|$ is the free-running, steady-state field magnitude, and $|A_i|$ is the magnitude of the injection field. ϕ is the phase difference between A and A_i. $\tilde{n} = (N/N_0 - 1)$, where N is the carrier density and N_0 is the steady-state carrier density of the free-running laser. G is the differental gain about the free-running, steady-state operating point,

$$G = \left[\frac{\gamma_c \gamma_n}{\gamma_s \tilde{J}}\tilde{n} - \gamma_p(2a + a^2)\right]. \quad (4)$$

γ_c, γ_n, γ_p, and γ_s are the photon decay rate, stimulated emission rate, gain saturation rate, and spontaneous carrier decay rate, respectively [7]. $\tilde{J} = (J/ed - \gamma_s N_0)/\gamma_s N_0$ is the pumping parameter, where J/ed is the carrier density injection rate, J is the injection current density, e is the electronic charge, and d is the active layer thickness. b is the linewidth enhancement factor, Ω is the frequency offset of the master laser from the free-running frequency of the slave laser, and η is the injection rate. F' and F'' are Langevin source terms for spontaneous-emission noise injected into the laser mode [8,9]. All input parameters required to numerically solve the set of coupled differential equations for a, ϕ, and $\tilde{n}$ can be determined experimentally [7].

In this work, we are specifically interested in the situation where the master laser is tuned to the frequency of the free-running slave laser, $\Omega = 0$. A linear stability analysis provides information about the resonant coupling between the carriers and the oscillating field. In Fig. 1, the non-zero eigenfrequency of the coupled equations is shown as a function of the injection parameter $\xi = (\eta|A_i|)/(\gamma_c|A_0|)$. The linear stability analysis predicts a bounded region of unstable dynamics and a monotonically increasing resonance frequency as the injection level is increased.

To understand the deterministic dynamics, the full nonlinear coupled equations are first solved with the noise

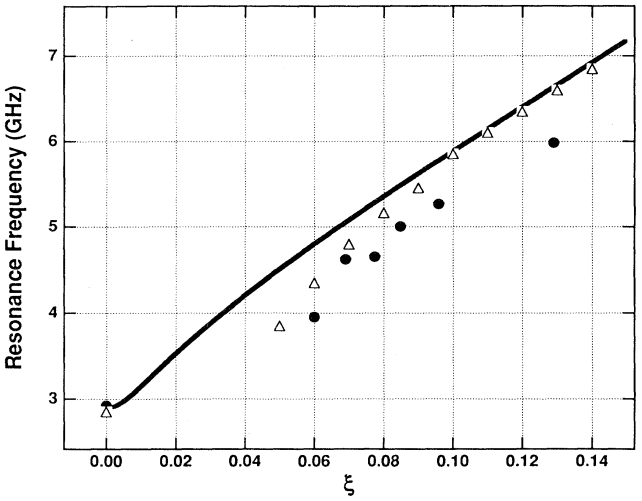

FIG. 1. Variation of the resonance frequency as a function of the injection level ξ. Solid line, calculation from the linear stability analysis. Triangles, fully nonlinear calculation. Bullets, experimental data. The model calculations used experimentally determined parameters for the slave laser operating at the same bias current as the data.

source terms set to zero. Figure 2 depicts the numerically obtained bifurcation diagram of the values of the extrema of the amplitude, $a(t)$, versus the injection parameter, ξ. As the injection level is increased, the steady state is destabilized and the relaxation frequency is undamped (Hopf bifurcation), in agreement with the linear stability analysis. Further increasing the injection leads to a period-doubling bifurcation route to chaos and then a similar, but reversed, route out of chaos. To confirm the chaotic nature, the Lyapounov exponents and the corresponding Kaplan-Yorke dimension of the attractor have been calculated [10]. For $\xi = 0.03$, the three Lyapounov exponents are $0.0145\gamma_c$, 0.0, and $-0.0298\gamma_c$, and the Kaplan-Yorke dimension is 2.48. The positive Lyapounov exponent is a clear measure that the system is chaotic in this parameter range. At even higher injection levels, the bifurcation diagram shows a second period doubling. Finally, at the highest injection levels, the laser diode reverts to stable operation (reverse Hopf bifurcation), consistent with the linear stability analysis.

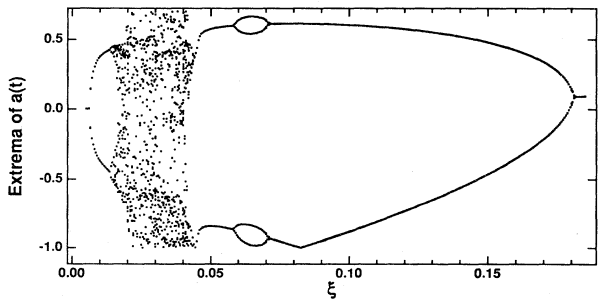

FIG. 2. Numerically calculated bifurcation diagram of the extrema of the normalized optical field amplitude $a(t)$ versus the normalized injection level ξ. Injection is at the free-running frequency of the slave laser. Experimentally determined parameters of the semiconductor laser are used in the calculation. The value of the linewidth enhancement factor is $b = 4$.

The experiments used commercially available, SDL-5301-G1, single-transverse and nearly single-longitudinal mode, GaAs/AlGaAs quantum well lasers. Approximately 90% of the output power is in the principal mode and none of the weak side modes contains more than 0.5%. Both the master and slave lasers were temperature and current stabilized. The optical frequencies of the two lasers could be matched to within ± 100 MHz. The master laser output was injected into the slave laser with careful alignment to ensure good coupling into the laser mode. Isolators were used to ensure that no light was injected back into the master laser. The output optical spectrum of the slave laser was monitored by a Newport SR-240C scanning Fabry-Perot with a free spectral range of 2 THz and a finesse of greater than 50 000. The dynamic parameters of the slave laser have been previously published [7]. Figures 1 and 2, and the data described below, correspond to the slave laser operating at an output level of 9 mW, where $\tilde{J} = 0.6$. A value of $b = 4$ was used in the calculations. At all but the highest injection levels investigated, the input noise due to spontaneous emission in the slave laser dominates the broadband noise spectrum of the master laser. The strength of the spontaneous emission was determined by comparing the relaxation resonance sidebands to the central peak of the free-running laser and using our model to relate the noise-source term to the steady-state intensity [9]. Likewise, to determine the injection level, we measured the spectrum in the weak injection limit and used our model to compare the generated sideband signal with the central peak [7].

Figure 3 shows six optical spectra of the principal mode of the slave laser taken with the injection at the free-running frequency. The frequency coordinate uses the free-running frequency or, equivalently, the injection frequency as the origin. The spectra illustrate operation in key regions of the bifurcation diagram (Fig. 2). In Fig. 3(a), $\xi = 0.014$, the spectrum consists of relatively narrow peaks separated by a frequency spacing of $f_r = 2.9$ GHz. These are typical features of highly unstable injection locking [11] and the spectrum is representative of the limit-cycle region above the first Hopf bifurcation. In Fig. 3(b), $\xi = 0.017$, broad period-doubling features appear in the spectrum between the narrow oscillation peaks and in Fig. 3(c), $\xi = 0.021$, the spectrum becomes dominated by a broad pedestal and many secondary peaks develop. These spectra illustrate the period-doubling route to chaos [3]. Within the region of chaotic dynamics, a fraction of the oscillating power, up to 35%, is shifted from the principal oscillating mode into several of the weak side modes. Over a narrow injection range, the broadened spectrum collapses again into narrow features with increased seperation, as shown in Fig. 3(d) where $\xi = 0.06$, and the principal mode regains its full power. This is consistent with the limit cycle in the bifucation diagram at injection levels just above the chaotic region. Also note the shift in the frequency coor-

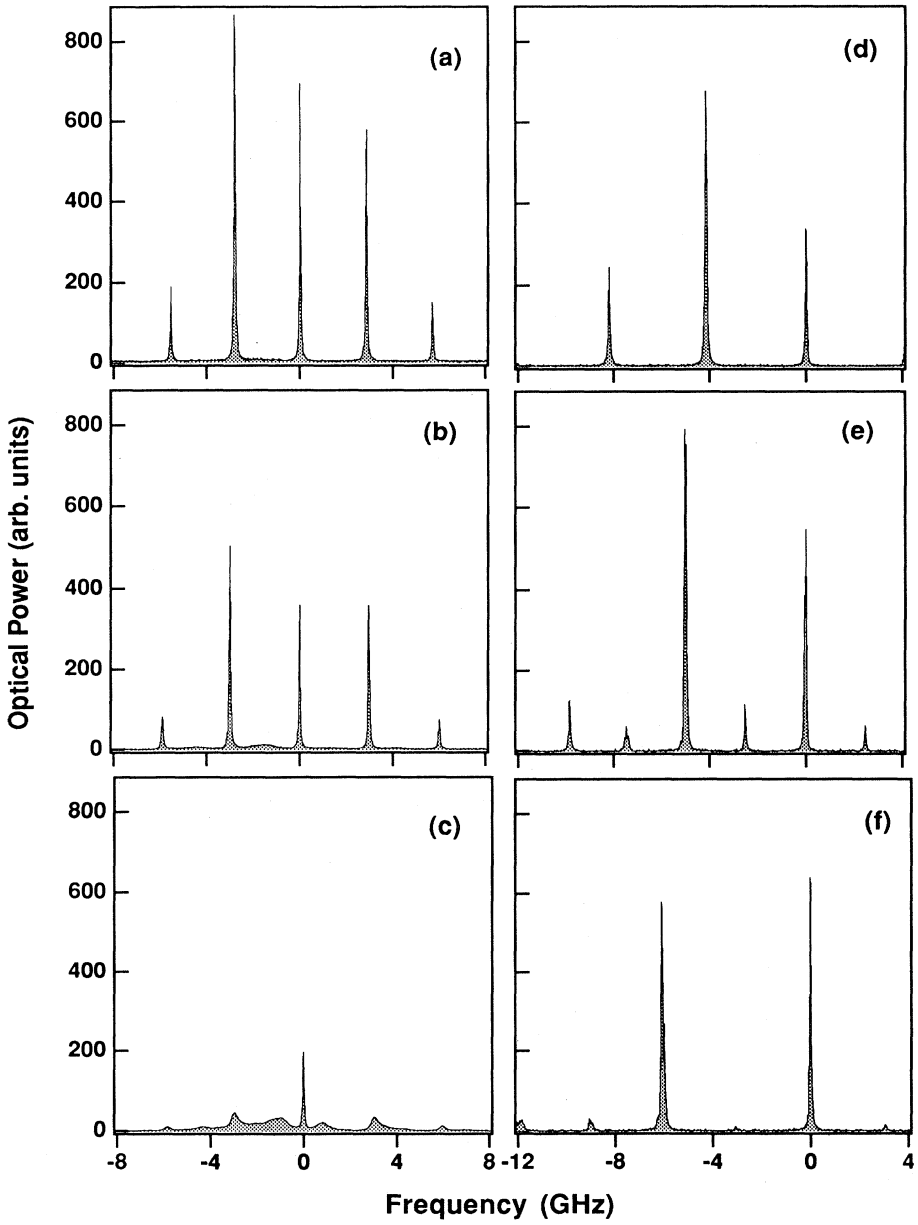

FIG. 3. Measured power optical spectra of the quantum well laser under optical injection at six levels of injection power: (a) unstable injection locking, limit cycle, at $\xi = 0.014$, (b) period doubling at $\xi = 0.017$, (c) chaotic dynamics at $\xi = 0.021$, (d) limit cycle at $\xi = 0.06$, (e) period doubling at $\xi = 0.085$, and (f) transition back to limit cycle at $\xi = 0.13$. Shading under the curves is a visual aid only. Note the shift of the frequency axis in (d), (e), and (f).

dinate and the strong asymmetry of the spectrum relative to the free-running/injection frequency. This asymmetry is present, to a lesser extent, in the low injection spectra and is due to the positive value of b [7]. At still higher injection levels, Fig. 3(e) where $\xi = 0.085$, a clear period doubling is observed with a further increase of the resonance frequency and relative strengthening of the negative frequency components. The period-doubling peaks then steadily decrease in magnitude as the injection is raised to $\xi = 0.13$, the largest value of injection that we were able to measure [Fig. 3(f)]. Just above this level the slave laser hopped to a new longitudinal mode. Up to the mode hop, we observe the major dynamical features represented in Fig. 2. The model also reproduces the observed increase in the resonance frequencies, as shown in Fig. 1.

When both coherent injection and spontaneous emission are present, there is, effectively, a fluctuating injected field. This leads to a blurring of the period-doubling cascades into and out of chaos. In the forward cascade, only the first period doubling is not obscured, and the new frequency components are severely broadened. The reverse cascade is completely obscured. This effect can be numerically recovered by including spontaneous-emission noise sources in the amplitude and phase equations. Figure 4 compares calculated spectra with and without the noise source terms at three injection levels. Without noise, a region of period doubling [Fig. 4(a)] and period quadrupling [Fig. 4(b)] are clearly distinguishable in the forward cascade. With noise, however, the calculations show only broadened period-doubling features [Figs. 4(d) and (e)] which are similar to

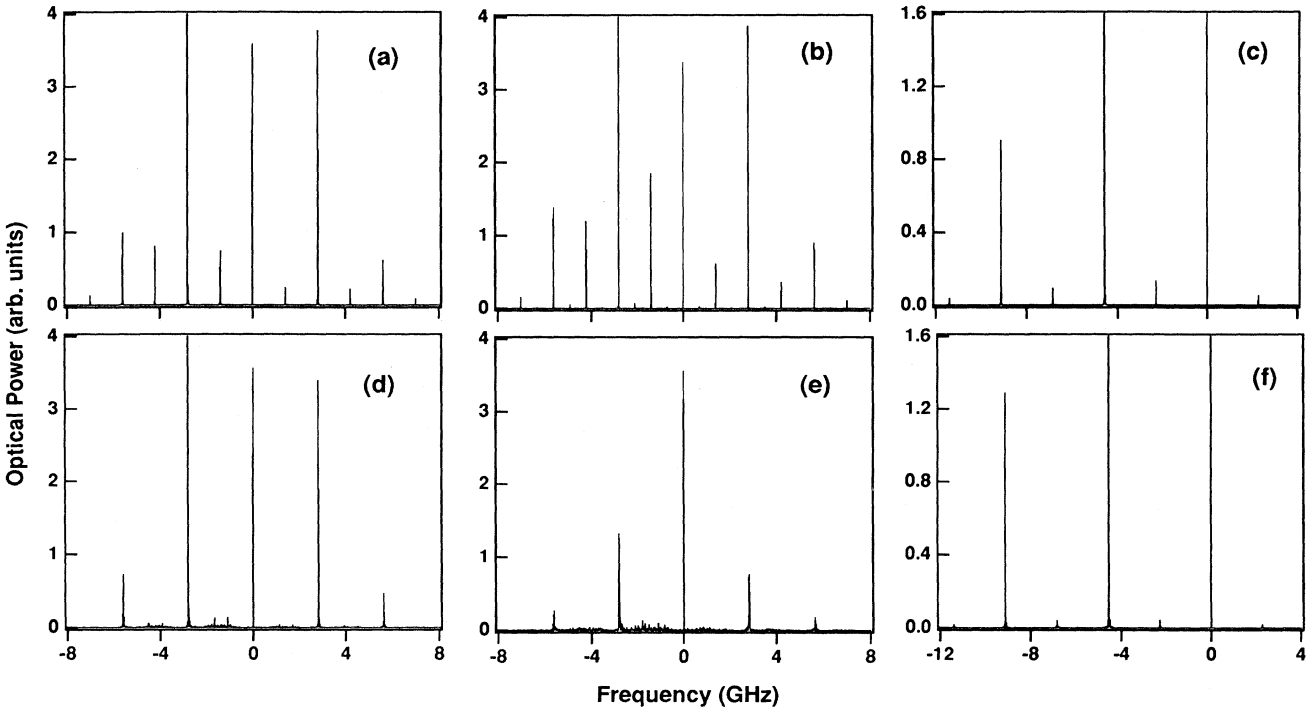

FIG. 4. Computed optical spectra showing the effects of the spontaneous-emission noise at three levels of injection. (a) and (d) $\xi = 0.0145$, (b) and (e) $\xi = 0.0152$, (c) and (f) $\xi = 0.064$. (d)–(f) include the spontaneous-emission noise source term while the others do not. The strongest spectral feature in (a), (b), and (d), and the two strongest in (c) and (f) are clipped to emphasize the detailed features. Note the shift of the frequency axis in (c) and (f).

the experimental data shown in Fig. 3(b). In the period-doubling bubble at higher injection levels, however, the noise does not severely broaden the new spectral peaks, as shown in Figs. 4(c) and (f). Likewise, the measured spectrum in Fig. 3(e) has sharp period doubling features.

Our observations of chaotic dynamics bounded by period-doubling cascades and a second, distinct region of period-doubled dynamics are similar to dynamics numerically generated using cubic maps and the biharmonically driven Duffing oscillator, and can occur in many dynamical systems with at least two control parameters [12]. In the semiconductor laser subject to external optical injection at its free-running frequency, the effective control parameters are the injection parameter ξ and the linewidth enhancement factor b. A region of chaotic dynamics bounded by period-doubling cascades has been observed in a CO_2 laser with modulated losses [13]. Alternating periodic and chaotic dynamics have been observed in driven, nonlinear $R-L$-diode circuits when the drive frequency is near-resonant to the circuit resonance or one of its subharmonics [14]. The equations which describe the biharmonically driven Duffing oscillator, the nonlinear electronic circuits, and the loss-modulated CO_2 laser have the common feature of an externally imposed modulation frequency. No external modulation frequencies are introduced in the dynamical equations (1)–(3) when the injection source oscillates at the same frequency as the free-running slave laser. There is, however, an effective detuning which is associated with the linewidth enhancement factor b. It represents an offset between the peak of the gain and the laser oscillation frequency [8,15]. By appropriately detuning the injection frequency, or by varying the value of b, one can observe completely different dynamics, including stable injection locking at all injection levels [2,3,11].

In conclusion, the excellent qualitative and good quantitative agreement between our experimental data and the calculations is strong evidence that Eqs. (1)–(3) capture the essential physics of a nearly single-mode laser subject to external optical injection, at least up to the point of the observed longitudinal mode hop. The model includes the dependence of the gain on both the carrier density and circulating field intensity. Within the region of chaotic dynamics, power is partitioned from the principal oscillating mode to the weak side modes and this cannot be recovered in the single-mode model. However, the partitioning does not appear to be a driving factor in the dynamics, given the good agreement between observed and calculated spectra. By suppressing the noise in the calculations, we are able to see that the model predicts dynamics similar to those predicted or observed in other physical systems. These dynamics are induced without introducing an external modulation frequency when the optical injection is at the free-running frequency of the semiconductor laser. This point emphasizes the critical role of the linewidth enhancement factor b in determining the nonlinear dynamics.

The authors wish to thank F. Doft for technical assistance. The work of T.B.S and J.M.L. was supported by the Air Force's Phillips Laboratory under Contract No. F29601-91-C-0081. P.M.A. would like to thank the National Research Council for support though an NRC Associateship.

[1] See, for example, *Nonlinear Dynamics in Optical Systems Technical Digest, 1992* (Optical Society of America, Washington, D.C., 1992), Vol. 16; Proc. SPIE **2039** (1994).

[2] J. Sacher, D. Baums, P. Panknin, W. Elsässer, and E. O. Göbel, Phys. Rev. A **45**, 1893 (1992).

[3] T. B. Simpson, J. M. Liu, A. Gavrielides, V. Kovanis, and P. M. Alsing, Appl. Phys. Lett. **64**, 3539 (1994).

[4] G. C. Dente, P. S. Durkin, K. A. Wilson, and C. E. Moeller, IEEE J. Quantum Electron. **24**, 2441 (1988).

[5] J. Mork, J. Mark, and B. Tromborg, Phys. Rev. Lett. **65**, 1999 (1990).

[6] T. B. Simpson, J. M. Liu, V. Kovanis, and A. Gavrielides, in *International Quantum Electronics Conference*, 1994 OSA Technical Digest Series Vol. 9 (Optical Society of America, Washington, D.C., 1994), p. 221.

[7] T. B. Simpson and J. M. Liu, J. Appl. Phys. **73**, 2587 (1993); J. M. Liu and T. B. Simpson, IEEE Photon. Technol. Lett. **4**, 380 (1993); IEEE J. Quantum Electron. **30**, 957 (1994).

[8] G. P. Agrawal and N. K. Dutta, *Long-Wavelength Semiconductor Lasers* (Van Nostrand Reinhold, New York, 1986) Chap. 6.

[9] T. B. Simpson, J. M. Liu, V. Kovanis, T. Gavrielides, and C. M. Clayton, Proc. SPIE **2039**, 23 (1993); T. B. Simpson and J. M. Liu, Opt. Commun. **112**, 43 (1994).

[10] E. Ott, *Chaos in Dynamical Systems* (Cambridge University Press, New York, 1993); T. S. Parker and L. O. Chua, *Practical Numerical Algorithms for Chaotic Systems* (Springer-Verlag, New York, 1989).

[11] I. Petitbon, P. Gallion, G. Debarge, and C. Chabran, IEEE J. Quantum Electron. **24**, 148 (1988).

[12] M. Bier and T. C. Bountis, Phys. Lett. A **104**, 239 (1985); G. L. Oppo and A. Politi, Phys. Rev. A **30**, 345 (1984).

[13] C. Lepers, J. Legrand, and P. Glorieux, Phys. Rev. A **43**, 2573 (1991).

[14] J. Cascais, R. Dilão, and A. Noronha da Casta, Phys. Lett. A **93**, 213 (1983), M. F. Bocko, D. H. Douglas, and H. H. Frutchy, *ibid.* **104**, 388 (1984); S. Tanaka, T. Matsumoto, J. Noguchi, and L. O. Chua, *ibid.* **157**, 37 (1991).

[15] J. R. Tredicce, F. T. Arecchi, G. L. Lippi, and G. P. Puccioni, J. Opt. Soc. Am. B **2**, 173 (1985).